Optical Coherence Tomography: Role in Percutaneous Coronary Intervention

12

David L. Ain, Robert Gallagher, and Ik-Kyung Jang

Abstract

Optical coherence tomography (OCT) is an imaging modality that utilizes back-reflection of near-infrared light. Superior resolution intra-coronary imaging, including assessment of plaque morphology and characteristics as well as imaging stents and post-stent complications have made OCT a powerful research tool, and more recently a clinical tool for guidance of PCI. Visualization of coronary lesions with OCT and their characterization as lipid-rich, fibrous, or fibro-calcific plaque can influence percutaneous coronary intervention (PCI) procedural planning. OCT has contributed significantly to the understanding of culprit lesion pathophysiology in acute coronary syndromes (ACS). ACS culprit lesions have been categorized by OCT features as resulting from plaque rupture, calcific nodule, or plaque erosion. Finally, OCT has proven to be an ideal imaging modality for ensuring optimal results after PCI. OCT can be used to assess for appropriate stent expansion and apposition of the stent with the vessel wall, and is an effective modality for the detection and assessment of stent-edge dissection, incomplete stent apposition, and in-stent tissue protrusion. The resolution of OCT allows for detection and assessment of in-stent neointima proliferation and neoatherosclerosis. A demonstrated safe and effective research instrument, OCT has shown great potential in this clinical role as an adjunctive imaging modality for PCI.

Keywords

Optical coherence tomography • Intra-coronary imaging • Acute coronary syndrome • Coronary artery disease • Intravascular ultrasound • Percutaneous coronary intervention • Plaque rupture • Calcific nodule • Plaque erosion • Instent restneosis • Neointimal proliferation • Neoatherosclerosis

Background

Optical coherence tomography (OCT) is an imaging modality that utilizes back-reflection of near-infrared light. OCT was initially developed at the Massachusetts Institute of Technology, and demonstrated ex vivo imaging of the retina as well as atherosclerotic plaque in 1991 [1]. Its intravascular use was subsequently developed in the late 1990s. For coronary imaging, OCT is performed using an intracoronary catheter that directs near-infrared light toward the coronary arterial walls and then measures the magnitude and echo time delay of the reflected light signal to generate an image. This is analogous to intravascular ultrasound

D.L. Ain, MD • R. Gallagher, MD
Cardiology Division, Massachusetts General Hospital, Boston, MA, USA
e-mail: dain@mgh.harvard.edu; rmgallagher@mgh.harvard.edu

I.-K. Jang, MD, PhD (✉)
Cardiology Division, Massachusetts General Hospital, Boston, MA, USA

Cardiology Division, Harvard Medical School, Boston, MA, USA
e-mail: ijang@mgh.harvard.edu

M.H. Picard et al. (eds.), *Intraprocedural Imaging of Cardiovascular Interventions*, DOI 10.1007/978-3-319-29428-5_12

(IVUS), which is being widely utilized in intracoronary imaging, except that OCT generates images by measuring the echo time delay and magnitude of backscattered light instead of sound [1]. OCT imaging has superior spatial resolution compared with IVUS, with current OCT systems providing an axial resolution of 10–15 μm and lateral resolution of 20–30 μm, but with tissue depth limited to 2–3 mm [2]. By comparison, IVUS has a spatial resolution of approximately 150–250 μm with tissue depth up to 10 mm [3]. A recently introduced Ilumien Optis OCT system utilizes a rapid automated pullback to image up to 75 mm coronary segments at a rate of 35 mm/s. OCT has been safely incorporated into cardiac catheterization procedures with low rates of complications [4]. Superior resolution coronary imaging, including assessment of plaque morphology and characteristics as well as imaging stents and post-stent complications have made OCT a powerful research tool, and more recently a clinical tool for guidance of percutaneous coronary interventions (PCI).

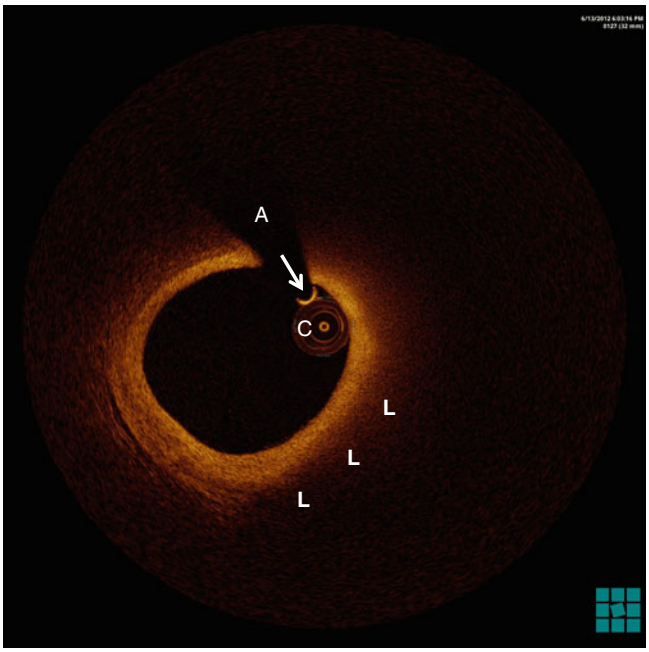

Fig. 12.1 Lipid-rich plaque (*L*) is characterized by a signal-poor region with diffuse borders. The OCT catheter (*C*) and coronary guidewire (*arrow*) can be seen within the artery lumen. The guidewire causes a backscatter imaging artifact (*A*) at the top of the image

OCT of Coronary Atherosclerosis

Practical application of OCT during coronary angiography in current cardiac catheterization procedures involves tracking of the OCT catheter into the coronary artery over a standard 0.014 in. coronary guidewire with image acquisition then performed during automated pullback of the imaging transducer within the OCT catheter. Because intraluminal blood produces significant scatter artifact on OCT images, image acquisition must be performed simultaneously with catheter injection of contrast, dextran, or saline to fully displace blood from the imaged coronary segments. For this reason, careful guiding catheter engagement for injection is critical to ensuring adequate image quality. Similarly, aorto-ostial segments of the left main and right coronary arteries are often difficult to adequately image with OCT, as imaging these locations prohibits full engagement of the guiding catheter, making displacement of blood by injection of these segments difficult. Once acquired, images are recorded and can be reviewed and manipulated in axial and longitudinal views to allow for analysis of the coronary anatomy and pathology, also facilitating measurements for guidance of PCI.

OCT has proven useful in identifying plaque characteristics with more accuracy and detail than other modalities, including IVUS [5–10]. Visualization of coronary lesions with OCT and their characterization as lipid-rich, fibrous, or fibro-calcific plaque (Figs. 12.1, 12.2, and 12.3) can

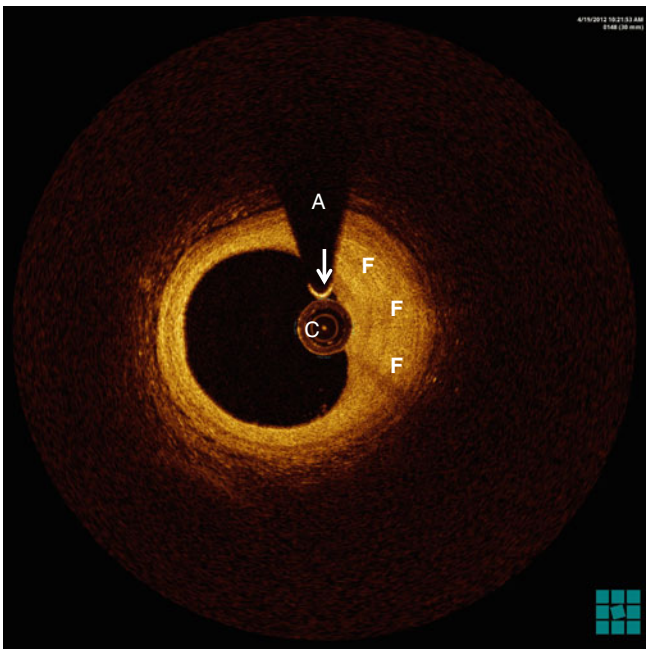

Fig. 12.2 Fibrous plaque (*F*) is characterized by a homogenous signal-rich region. Again, the OCT catheter (*C*) and coronary guidewire (*arrow*) can be seen within the artery lumen, with the guidewire causing characteristic backscatter imaging artifact (*A*)

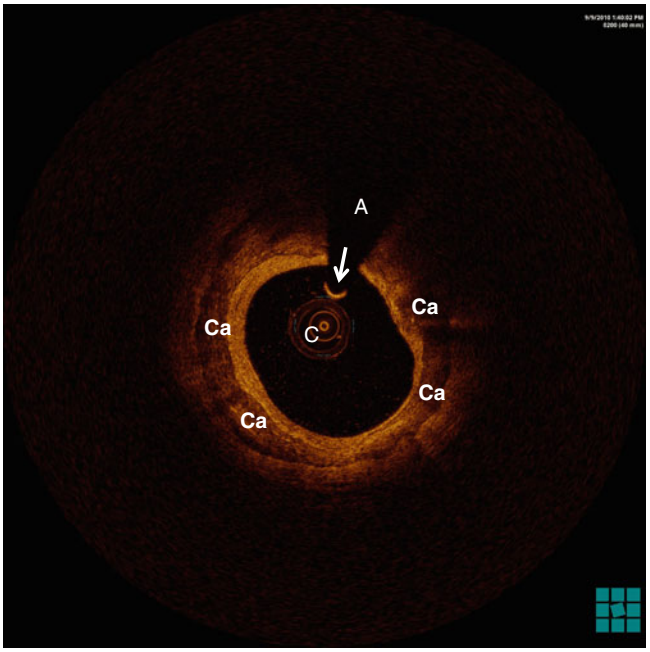

Fig. 12.3 Fibrocalcific plaque (*Ca*) is characterized by well-delineated, signal-poor regions with sharp borders. Circumferential calcification is seen in this image. Again, the OCT catheter (*C*) and coronary guidewire (*arrow*) can be seen within the artery lumen, with the guidewire causing characteristic backscatter imaging artifact (*A*)

influence PCI procedural planning. Furthermore, OCT has contributed significantly to the understanding of culprit lesion pathophysiology in acute coronary syndromes (ACS). ACS culprit lesions have been categorized by OCT features as resulting from plaque rupture, calcific nodule, or plaque erosion. Thrombus associated with culprit lesions is well visualized by OCT and can be characterized as platelet rich white thrombus or platelet poor red thrombus based on backscatter and attenuation characteristics (Fig. 12.4). Other non-traditional causes of ACS culprit lesions can also be well characterized by OCT. These include spontaneous coronary artery dissection, mural hematoma, and recanalized thrombus.

Although still primarily an area of research with a yet undefined clinical role, OCT imaging of vulnerable coronary plaques has been a vibrant area of research and discovery. Vulnerable plaques are those that have a high risk of rupture and resultant ACS. Histologic features of such vulnerable plaques include thin fibrous caps (<65 μm), large lipid cores (more than 40 % of overall plaque volume), and increased macrophage infiltration. OCT, with its resolution of 10–15 μm, is the only modality capable of visualizing the thin fibrous cap for identification of a thin cap fibroatheroma (TCFA) (Fig. 12.5). OCT identification of TCFA has been

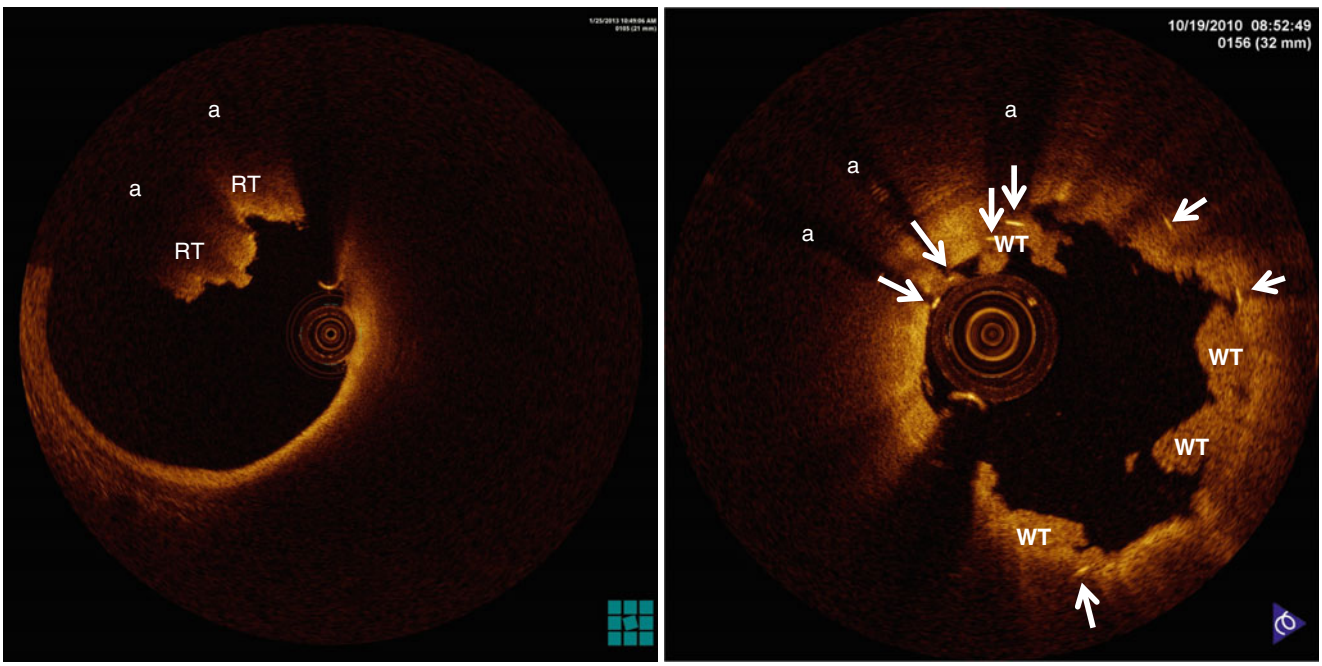

A: Red Thrombus **B: White Thrombus**

Fig. 12.4 Thrombus is clearly visible by OCT. (**a**) Red thrombus (*RT*) is erythrocyte-rich, platelet-poor and has a high degree of backscattering and attenuation (**a**). (**b**) White thrombus (*WT*) is platelet-rich and has homogenous backscatter and low attenuation. Structure including stent struts is visible behind thrombus. Metallic stent struts (*arrows*) are clearly visible and produce characteristic attenuation artifact (**a**)

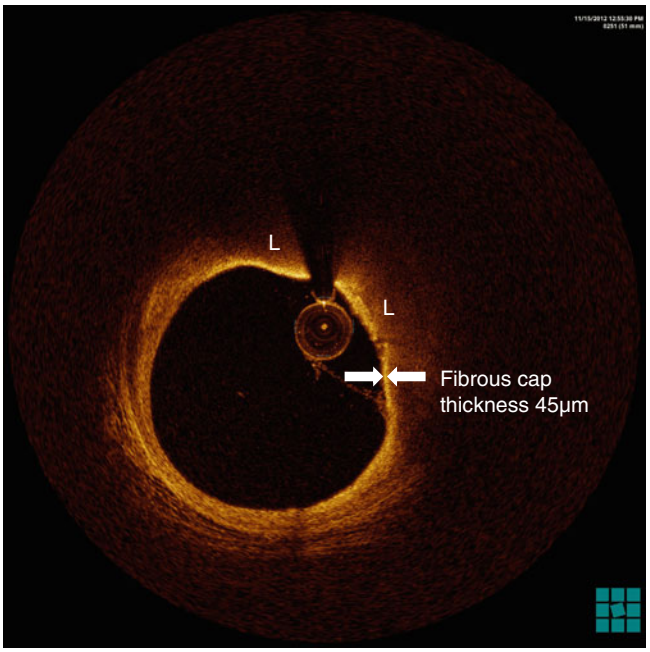

Fig. 12.5 Thin-cap fibroatheroma is characterized by a large lipid core (*L*) under a thin fibrous cap of <65 μm thickness

shown to correlate well with histology [11, 12]. Clinically correlated, patients with ACS are significantly more likely to have disrupted thin fibrous caps overlying their culprit lesions and thinner mean cap thickness compared with patients presenting with stable angina [9, 13].

OCT-Guided PCI

Before PCI, OCT can be used to accurately determine target vessel and lesion dimensions and characteristics to inform optimal stent sizing and procedural execution. If possible, OCT imaging can be performed prior to any manipulation of the target lesion, other than guidewire passage. In the event of a very severe stenosis or occlusive thrombus precluding OCT catheter passage, gentle balloon angioplasty pre-dilation can be performed to allow passage of the OCT catheter without gross disruption of the lesion if possible. Pre-PCI imaging is used to measure reference vessel diameter both proximal and distal to the target lesion, as well as lesion length (Fig. 12.6). These measurements are used to determine stent sizing, and a phantom-controlled study comparing OCT to IVUS for measurement of luminal dimensions found that OCT was more accurate and more reproducible than IVUS for making these measurements [14]. Lesion and reference vessel measurements are then used to select optimal stent diameter and length as well as appropriately size pre-dilation and post-dilation angioplasty balloons.

Plaque characteristics such as fibrous, lipid content and degree of calcification can also be determined on pre-PCI OCT imaging. These characteristics, as defined by OCT correlate with the risk of post-PCI complications [15–18]. These features may further influence choices regarding lesion preparation prior to stenting (i.e. use of pre-dilatation, cutting balloon, rotational atherectomy, etc.).

Minimal luminal area (MLA) of the target lesion can also be determined by OCT prior to any intervention (Fig. 12.6). OCT-derived MLA is moderately accurate, using fractional flow reserve (FFR) as the gold standard, in determining lesion severity, and similar in accuracy to IVUS [19]. OCT, although sensitive in this regard, has lower specificity and therefore limited positive predictive value for defining severe stenoses [20].

OCT for the Detection of Post-PCI Complications

While steady advances in PCI techniques and stent technology—including composition, design, and pharmacology—have made the field of interventional cardiology remarkably safe and effective, complications related to stent placement continue to limit procedural success in certain cases [21]. Understanding the mechanisms behind stent thrombosis and restenosis provides a potential opportunity to alter procedural elements in order to prevent adverse events. Intracoronary imaging has emerged as a key element in both defining stent complications and attempting to prevent untoward outcomes related to stenting. Research utilizing IVUS has laid the groundwork for this understanding, and IVUS has been the predominant mode of this type of imaging in clinical practice [22–27]. With its higher resolution and sensitivity, OCT has however emerged as an attractive modality for the characterization of both acute and chronic complications of intracoronary stenting.

Over the past decade, several studies have examined the feasibility of OCT for the detection of complications that arise post-PCI [28–31], and additional work has explored the connection between OCT-identified complications and adverse cardiac events [32]. OCT has proven to be an ideal imaging modality for ensuring appropriate stent expansion and evaluating apposition of the stent with the vessel wall [33, 34]. In addition to being an accurate tool for the evaluation of stent expansion and stent-vessel apposition, OCT has been demonstrated to be an effective modality for the detection and assessment of stent-edge dissection (disruption of the intima) (Fig. 12.7) [28, 30, 31, 35], incomplete stent apposition [28, 34] (Fig. 12.8), and in-stent tissue protrusion (protrusion of tissue between stent struts) [32, 36] (Fig. 12.9). More recent work has focused on the clinical implications of

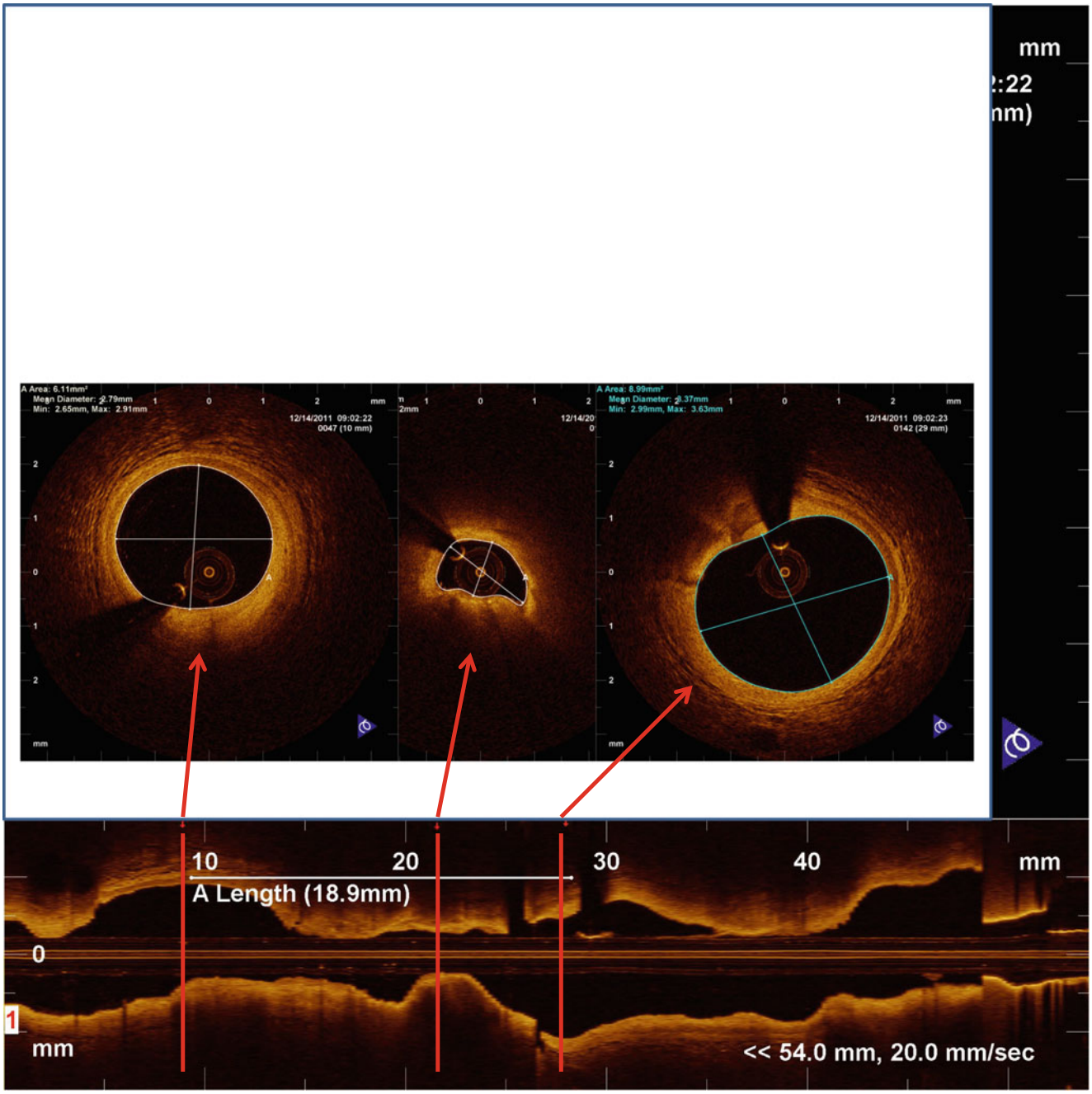

Fig. 12.6 OCT-guided PCI: lesion length is measured using the longitudinal view (*bottom*) and proximal (*right*) and distal (*left*) reference vessel diameters as well as MLA (*center*) are measured in the axial views. In this case the mean proximal reference vessel diameter is 3.37 mm and mean distal reference vessel diameter is 2.79 mm, with an MLA of 1.41 mm^2. Lesion length is 18.9 mm. Based on these OCT measurements, appropriate PCI for this lesion consisted of deployment of a 2.75 × 20 mm stent, followed by post-dilation to 3.5 mm in the proximal segment

OCT-identified complications that arise after PCI [37], and sought to identify stent complications that are associated with increased rates of adverse outcomes [32].

Measurement of minimal stent area is an important assessment that can be made with intravascular imaging. Accurate stent area measurements have been made with greater ease using OCT due to its high resolution and some system features such as automatic edge detection. There appears to be a clear association between small minimal stent area and restenosis [22–24], and stent underexpansion has been found to be an independent predictor of major adverse cardiac events and target lesion revascularization [32]. Research done with IVUS led to a range of cutoff values of 5.0–5.7 mm^2 to predict restenosis. A recent study of OCT-defined acute stent complications, the largest to date, found the best minimal lumen cutoff to predict

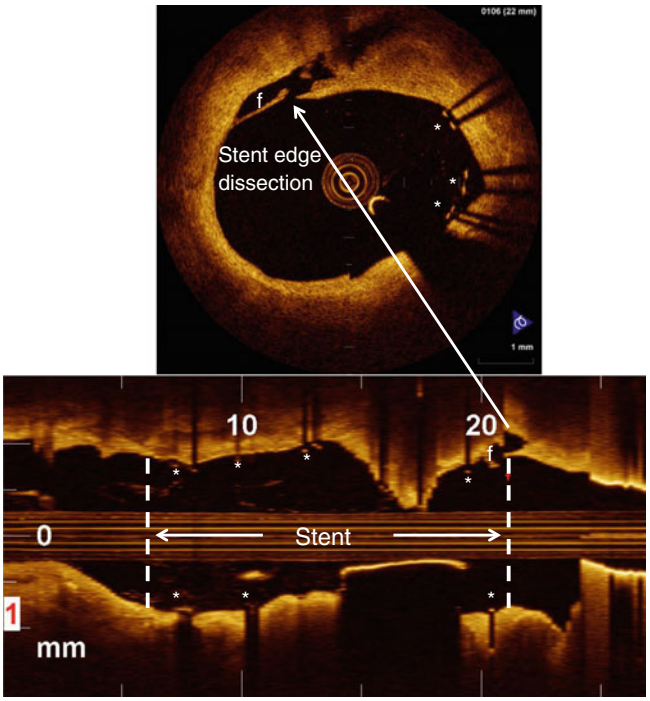

Fig. 12.7 Dissection flap (*f*) clearly visualized by OCT at the edge of a stent, both in the longitudinal view (*bottom*) and axial image (*top*). Groups of stent struts (*) are clearly seen in both views, with their characteristic attenuation artifact

target lesion revascularization by OCT is 5.0 mm^2, and smaller values were independent predictors of both major adverse cardiac events (MACE) and target lesion revascularization (TLR) [32].

Malapposition of the stent with the arterial wall is seen by OCT in anywhere from 10 % to 70 % of stents post-implantation [31–33], and incomplete apposition has been associated with late stent thrombosis [38–40]. OCT permits visualization of individual stent struts and determination of the distance of each strut from the vessel [33]. Research using OCT has demonstrated that reendothelialization occurs more slowly when stent struts are malapposed with the vessel wall [41]. Given what is known about the role of endothelialization in reducing exposure of the thrombogenic surface of the stent polymer and thereby preventing stent thrombosis, the effect of malapposition on late stent thrombosis may be a crucial one. Fortunately new stent scaffolds and enhanced antiplatelet therapy have drastically decreased the rate of serious adverse events after PCI; this will, however, make identifying technical factors that contribute significantly to clinical outcomes more difficult.

OCT's high image resolution allows for identification of dissections at the stent edge and within the stented segment. Because of the higher resolution, stent-edge

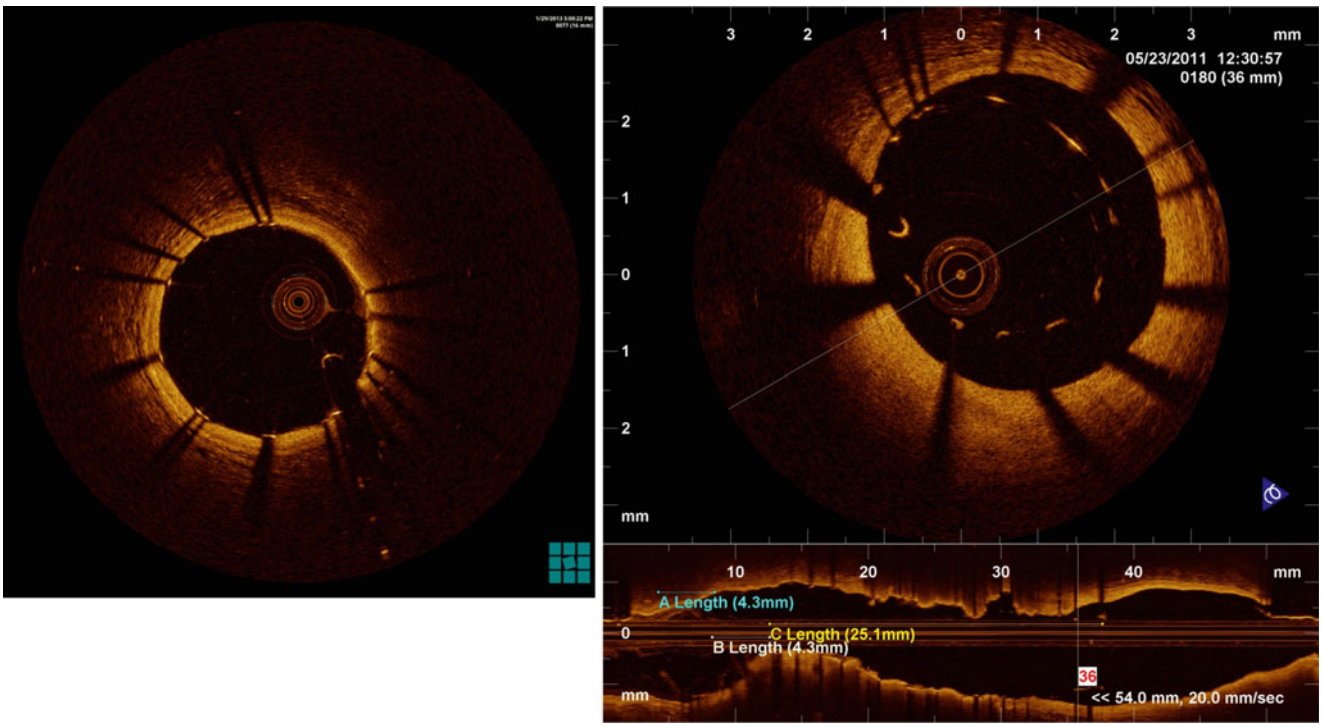

Fig. 12.8 (*Left*) A well-apposed stent with all struts in contact with the coronary intima. (*Right*) Malapposed stent struts with significant distance from the intima. Struts >320–350 μm from the intima are unlikely to become endothelialized and may be associated with adverse coronary events

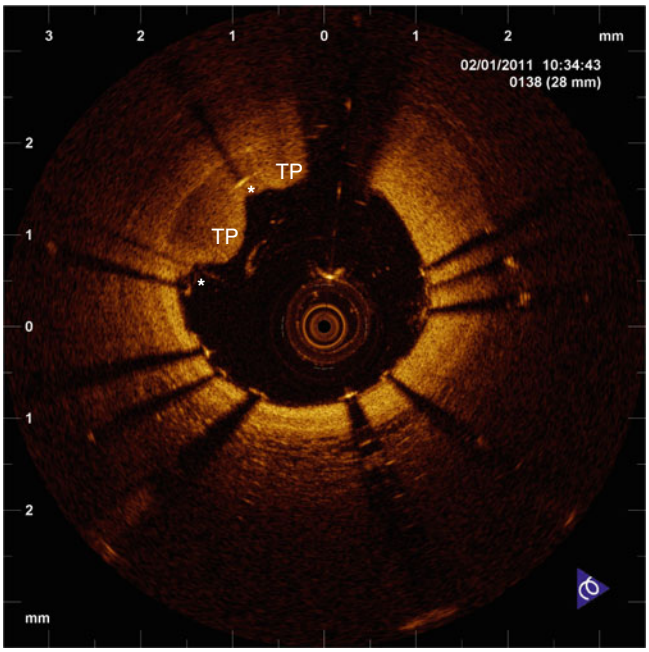

Fig. 12.9 In-stent tissue protrusion (*TP*) between stent struts (*)

dissection (SED) is found at least twice as often by OCT compared with IVUS [28, 31, 35]. OCT-detected SED is less likely to occur when the stent is expanded with its edge in a normal segment of artery compared with in an atherosclerotic plaque [42]. Additional research suggests that the type of plaque that the stent edge is placed in directly affects the risk of SED, with lipid and calcified plaques posing a much higher risk than fibrous plaques [29, 32]. While several studies have not shown a relationship between SED or in-stent dissection and clinical events [31, 32, 37, 43], the amount of lipid at the proximal stent edge has been shown to correlate with post-PCI creatinine kinase-MB elevation [44].

One under-investigated application of OCT is the detection and characterization of in-stent tissue prolapse or protrusion. Recent work suggests that when tissue protrusion is evaluated by OCT, the appearance of the protrusion correlates with the severity of vessel injury. Irregular protusion, suggesting moderate to severe vessel injury, was found to be an independent predictor of MACE and TLR.

Finally, OCT has the ability to identify thrombus within stents [45] (Fig. 12.4b). While the clinical significance of incidentally-discovered thrombus is unclear, it was found to be associated with longer stent length, smaller stent diameter, and absence of neointimal formation over stent struts. In general, small amounts of incidentally discovered in-stent thrombus need not prompt thrombus aspiration in the setting of good angiographic flow, but may influence the intensity of anti-thrombotic therapy.

Neointimal Hyperplasia and Neoatherosclerosis

The tendency of a neointima—composed of smooth muscle cells and extracellular matrix—to form within stents has been appreciated for years; indeed its presence is a surrogate for stent failure and vessel loss. The resolution of OCT allows for detection of neointima below the threshold of IVUS (Fig. 12.10). Three patterns of neointima have been described, based on the appearance by OCT: homogeneous (Fig. 12.11), heterogeneous (Fig. 12.12), and layered (Fig. 12.13) [46]. Small case series and case reports suggest that these OCT patterns of neoitima have histopathologic correlates, with the homogenous pattern identifying tissue with abundant smooth muscle cells and the other patterns signalizing extracellular matrix [47, 48].

In the last several years, post-mortem examination of coronary stents has demonstrated that atherosclerotic change within the neointima is a frequent occurrence, and it occurs earlier and nearly twice as often, in drug-eluting (DES), compared with bare metal stents (BMS) [49]. Neoatherosclerosis is a discrete pathologic process in which, months or years after stent implantation, foamy macrophages coalesce in the neointima around stent struts [31, 32]. When this process takes hold, these areas of neoatherosclerosis appear to be subject to the same fates as atherosclerotic plaques in native vessels. Calcium deposition occurs, as does formation of necrotic cores, leading to regions vulnerable to rupture and thrombosis [52]. This is a key mechanism underlying very late stent failure. Work has shown that neoatherosclerosis can be detected by OCT, and OCT has demonstrated that over time the neointima transforms into a lipid-rich tissue [50, 51] (Fig. 12.14). OCT-based research has corroborated the pathologic findings of earlier neoatherosclerosis with drug-eluting stents, but found that after 2 years, its frequency was the same in both drug-eluting and bare metal stents [53]. While evidence implicates incomplete endothelialization in late stent thrombosis, plaque rupture in the neointima has emerged as another mechanism. In the modern era of PCI, late stent thrombosis is a rare event, but a complete understanding of its pathogenesis may help avert this catastrophic occurrence. The degree of resolution afforded by OCT makes it an ideal modality for examining neointimal formation and assessing neoatherosclerosis.

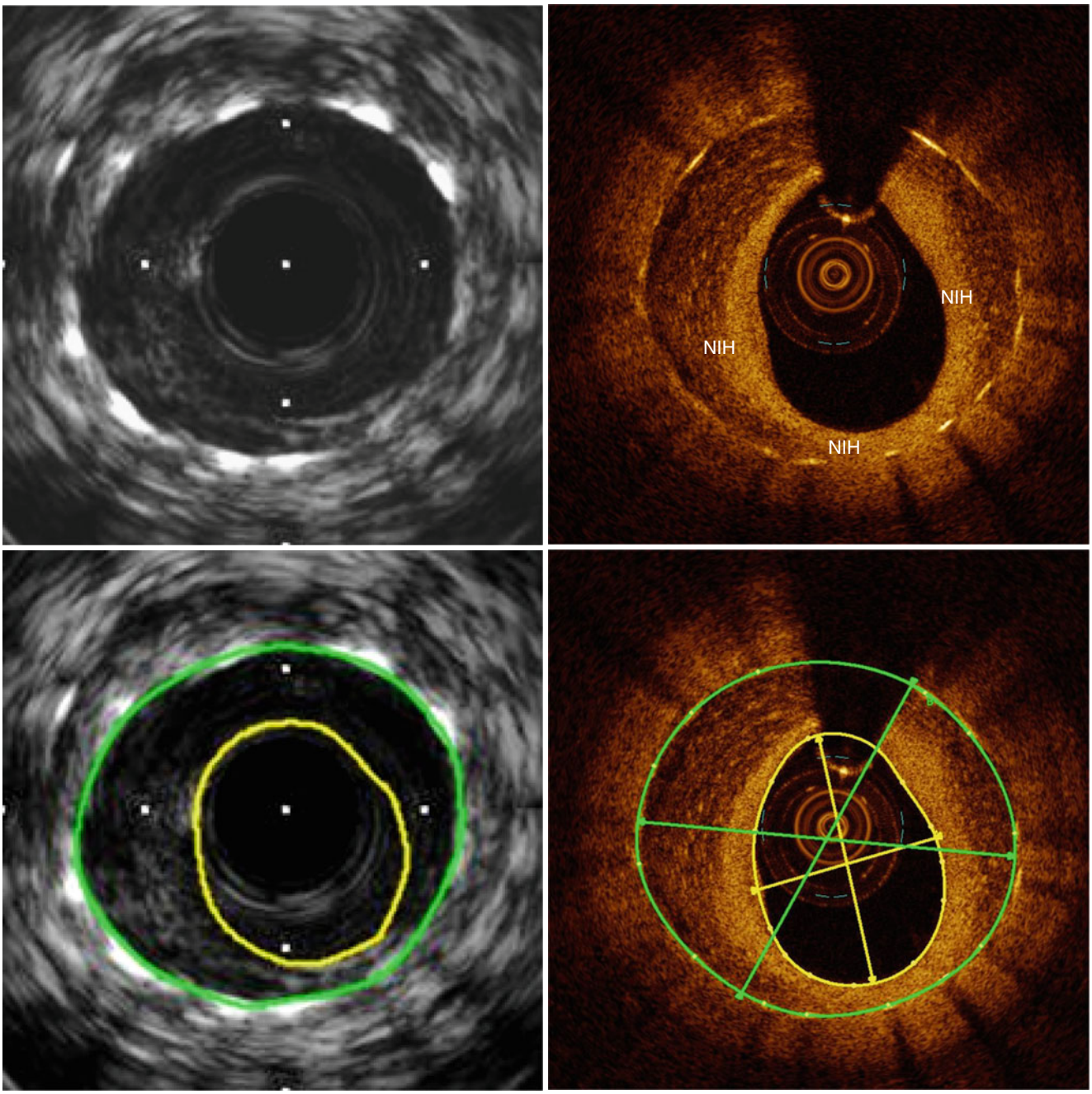

Fig. 12.10 Neointimal hyperplasia (*NIH*) within a stent is more clearly visualized by OCT (*right*) vs. IVUS (*left*), allowing more detailed tissue characterization as well as luminal and stent measurements (*bottom*)

OCT Evaluation of Bioabsorbable Vascular Scaffolds

Ongoing research has focused on the potential for a bioabsorbable vascular scaffold (BVS) to replace DES for intracoronary stenting. Because it is eventually absorbed, leaving no foreign body in the artery, BVS may reduce the risk of late stent thrombosis and other complications of PCI. Both animal and human outcomes studies have used intravascular imaging, including OCT, to evaluate the absorption of the polymer and the repopulation of BVS sites with cells. BVS currently under investigation appear different from metallic stents when imaged with IVUS; the struts are translucent, and OCT can completely image the strut thickness as well as the arterial wall behind the scaffold [54]. While BVS struts were no longer recognizable by IVUS after 2 years, some

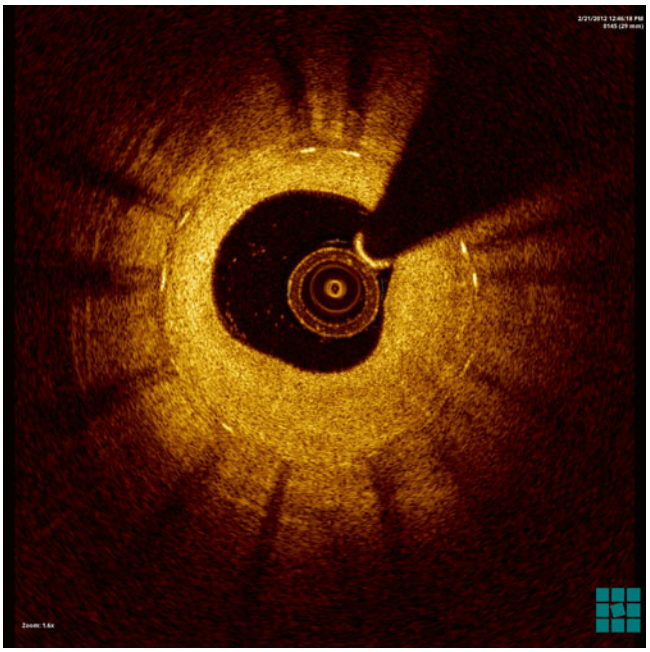

Fig. 12.11 Homogeneous neointimal hyperplasia

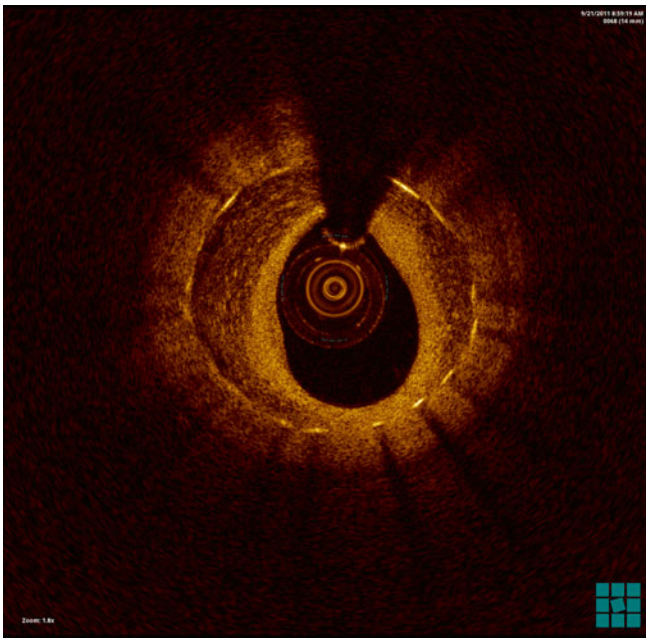

Fig. 12.13 Layered neointimal hyperplasia. The inner layer has high intensity signal, whereas the outer layer shows low signal material

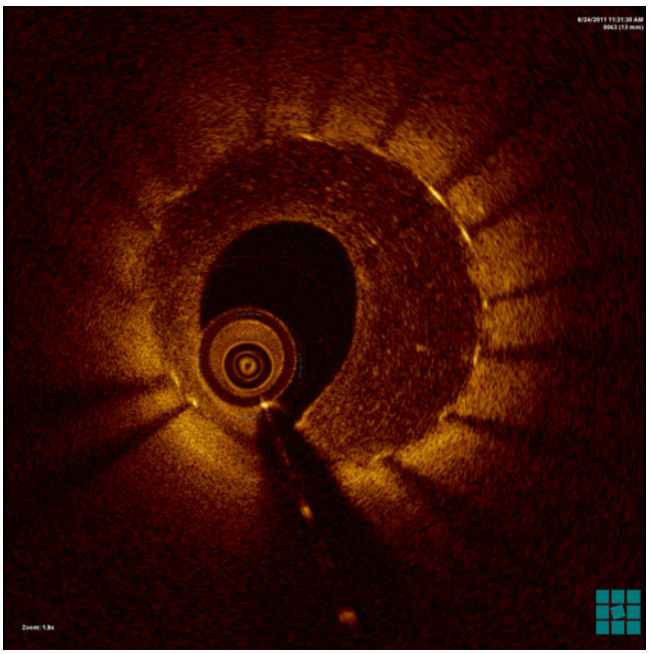

Fig. 12.12 Hetergeneous neointial hyperplasia

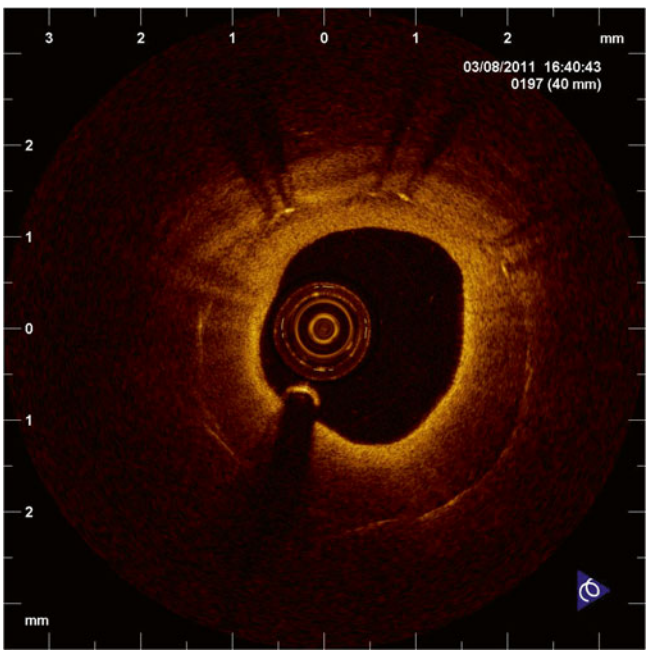

Fig. 12.14 Neoatherosclerosis within a coronary stent as characterized by OCT appears as a signal-poor regions (lipid laden) within stent struts

strut signals appeared to persist on OCT imaging in two thirds of cases. OCT was able to demonstrate a homogenous vessel wall at the site of the scaffold, suggesting endothelial healing [55]. Recent investigation employing serial OCT evaluation showed that, unlike BMS, self-expanding BVS expand over time, resulting in larger vessel diameters and preserved lumen size [56]. Potential applications of OCT continue to evolve with advances in both OCT technology

and stent design. Work with three-dimensional OCT has demonstrated the ability of reconstructions using this technology to evaluate vessel side branches jailed by BVS [57].

Conclusions

OCT is a safe and easily employed intravascular imaging modality with unmatched resolution and image quality of the coronary arteries. It has generated significant interest as a research tool for the evaluation of coronary vascular biology and atherosclerosis pathophysiology, but only recently has started to emerge into routine clinical practice for optimization of PCI. OCT shows great potential in this clinical role as an adjunctive modality for PCI, but is currently limited by the lack of clinical outcomes data supporting its routine clinical use. Similarly, routine IVUS-guided PCI had not been shown to improve hard clinical endpoints until recent meta-analysis of IVUS-guided DES implantation demonstrated significantly fewer adverse end points including death and MI in the IVUS-guided PCI group [40]. As OCT provides similar and possibly superior structural information upon which to guide PCI it may be reasonable to hypothesize that OCT-guided PCI may have similar clinical benefit. This has, however, yet to be rigorously studied and further outcome studies of OCT-guided PCI will be needed to differentiate the role of this promising technology in our clinical practice.

References

1. Huang D, Swanson EA, Lin CP, Schuman JS, Stinson WG, Chang W, et al. Optical coherence tomography. Science. 1991;254:1178–81.
2. Herrero-Garibi J, Cruz-Gonzalez I, Parejo-Diaz P, Jang IK. Optical coherence tomography: its value in intravascular diagnosis today. Rev Esp Cardiol. 2010;63:951–62.
3. Suh WM, Seto AH, Margey RJ, Cruz-Gonzalez I, Jang IK. Intravascular detection of the vulnerable plaque. Circ Cardiovasc Imaging. 2011;4:169–78.
4. Barlis P, Gonzalo N, Di Mario C, Prati F, Buellesfeld L, Rieber J, Dalby MC, Ferrante G, Cera M, Grube E, et al. A multicentre evaluation of the safety of intracoronary optical coherence tomography. EuroIntervention. 2009;5:90–5.
5. Suter MJ, Nadkarni SK, Weisz G, et al. Intravascular optical imaging technology for investigating the coronary artery. J Am Coll Cardiol Img. 2011;4:1022–39.
6. Low AF, Kawase Y, Chan YH, et al. In vivo characterization of coronary plaques with conventional grey-scale intravascular ultrasound: correlation with optical coherence tomography. EuroIntervention. 2009;4:626–32.
7. Kawasaki M, Bouma BE, Bressner J, et al. Diagnostic accuracy of optical coherence tomography and integrated backscatter intravascular ultrasoundimages for tissue characterization of human coronary plaques. J Am Coll Cardiol. 2006;48:81–8.
8. Garcia-Garcia HM, Gonzalo N, Regar E, et al. Virtual histology and optical coherence tomography: from research to broad clinical application. Heart. 2009;95:132–1374.
9. Kubo T, Imanishi T, Takarada S, et al. Assessment of culprit lesion morphology in acute myocardial infarction: ability of optical coherence tomography compared with intravascular ultrasound and coronary angioscopy. J Am Coll Cardiol. 2007;50:933–9.
10. Takano M, Jang IK, Inami S, et al. In vivo comparison of optical coherence tomography and angioscopy for the evaluation of coronary plaque charactistics. Am J Cardiol. 2008;101:471–6.
11. Kume T, Akasaka T, Kawamoto T, Okura H, Watanabe N, Toyota E, Neishi Y, Sukmawan R, Sadahira Y, Yoshida K. Measurement of the thickness of the fibrous cap by optical coherence tomography. Am Heart J. 2006;152(755):e751–4.
12. Raffel OC, Akasaka T, Jang IK. Cardiac optical coherence tomography. Heart. 2008;94:1200–10.
13. Jang IK, Tearney GJ, MacNeill B, Takano M, Moselewski F, Iftima N, Shishkov M, Houser S, Aretz HT, Halpern EF, et al. In vivo characterization of coronary atherosclerotic plaque by use of optical coherence tomography. Circulation. 2005;111:1551–5.
14. Kubo T, Takashi A, Shite J, et al. OCT compared with IVUS in a coronary lesion assessment. J Am Coll Cardiol Img. 2013;6:1095–104.
15. Yonetsu T, Kakuta T, Lee T, Takahashi K, Yamamoto G, Iesaka Y, Fujiwara H, Isobe M. Impact of plaque morphology on creatine kinase-MB elevation in patients with elective stent implantation. Int J Cardiol. 2011;146:80–5.
16. Lee T, Kakuta T, Yonetsu T, Takahashi K, Yamamoto G, Iesaka Y, Fujiwara H, Isobe M. Assessment of echo-attenuated plaque by optical coherence tomography and its impact on post-procedural creatine kinase-myocardial band elevation in elective stent implantation. JACC Cardiovasc Interv. 2011;4:483–91.
17. Lee T, Yonetsu T, Koura K, Hishikari K, Murai T, Iwai T, Takagi T, Iesaka Y, Fujiwara H, Isobe M, et al. Impact of coronary plaque morphology assessed by optical coherence tomography on cardiac troponin elevation in patients with elective stent implantation. Circ Cardiovasc Interv. 2011;4:378–86.
18. Porto I, Di Vito L, Burzotta F, Niccoli G, Trani C, Leone AM, Biasucci LM, Vergallo R, Limbruno U, Crea F. Predictors of periprocedural (type IVa) myocardial infarction, as assessed by frequency-domain optical coherence tomography. Circ Cardiovasc Interv. 2012;5:89–96. S81–86.
19. Gonzalo N, Escaned J, Alfonso F, Nolte C, Rodriguez V, Jimenez-Quevedo P, Banuelos C, Fernandez-Ortiz A, Garcia E, Hernandez-Antolin R, et al. Morphometric assessment of coronary stenosis relevance with optical coherence tomography: a comparison with fractional flow reserve and intravascular ultrasound. J Am Coll Cardiol. 2012;59:1080–9.
20. Stefano GT, Bezerra HG, Attizzani G, Chamie D, Mehanna E, Yamamoto H, Costa MA. Utilization of frequency domain optical coherence tomography and fractional flow reserve to assess intermediate coronary artery stenoses: conciliating anatomic and physiologic information. Int J Cardiovasc Imaging. 2011;27:299–308.
21. Garg S, Serruys PW. Coronary stents: current status. J Am Coll Cardiol. 2010;56(56):S1–42.
22. Choi SY, Witzenbichler B, Maehara A, Lansky AJ, Guagliumi G, Brodie B, et al. Intravascular ultrasound findings of early stent thrombosis after primary percutaneous intervention in acute myocardial infarction: a Harmonizing Outcomes with Revascularization and Stents in Acute Myocardial Infarction (HORIZONS-AMI) substudy. Circ Cardiovasc Interv. 2011;4(3):239–47.
23. Sonoda S, Morino Y, Ako J, Terashima M, Hassan AH, Bonneau HN, et al. Impact of final stent dimensions on long-term results following sirolimus-eluting stentimplantation: serial intravascular ultrasound analysis from the sirius trial. J Am Coll Cardiol. 2004;43(11):1959–63.

24. Hong MK, Mintz GS, Lee CW, Park DW, Park KM, Lee BK, et al. Late stent malapposition after drug-eluting stent implantation: an intravascular ultrasound analysis with long-term follow-up. Circulation. 2006;113(3):414–9.
25. Doi H, Maehara A, Mintz GS, Yu A, Wang H, Mandinov L, et al. Impact of post-intervention minimal stent area on 9-month follow-up patency of paclitaxel-eluting stents: an integrated intravascular ultrasound analysis from the TAXUS IV, V, and VI and TAXUS ATLAS workhorse, long lesion, and direct stent trials. JACC Cardiovasc Interv. 2009;2(12):1269–75.
26. Fujii K, Carlier SG, Mintz GS, Yang YM, Moussa I, Weisz G, et al. Stent underexpansion and residual reference segment stenosis are related to stent thrombosis after sirolimus-eluting stent implantation: an intravascular ultrasound study. J Am Coll Cardiol. 2005; 45(7):995–8.
27. Song HG, Kang SJ, Ahn JM, Kim WJ, Lee JY, Park DW, et al. Intravascular ultrasound assessment of optimal stent area to prevent in-stent restenosis after zotarolimus-, everolimus-, and sirolimus-eluting stent implantation. Catheter Cardiovasc Interv. 2014;83(6): 873–8.
28. Kume T, Okura H, Miyamoto Y, Yamada R, Saito K, Tamada T, et al. Natural history of stent edge dissection, tissue protrusion and incomplete stent apposition detectable only on optical coherence tomography after stent implantation: preliminary observation. Circ J. 2012;76:698–703.
29. Gonzalo N, Serruys PW, Okamura T, Shen ZJ, Garcia-Garcia HM, Onuma Y, et al. Relation between plaque type and dissections at the edges after stent implantation: an optical coherence tomography study. Int J Cardiol. 2011;150:151–5.
30. Gonzalo N, Serruys PW, Okamura T, Shen ZJ, Onuma Y, Garcia-Garcia HM, et al. Optical coherence tomography assessment of the acute effects of stent implantation on the vessel wall: a systematic quantitative approach. Heart. 2009;95:1913–9.
31. Kubo T, Imanishi T, Kibata H, Kuroi A, Ueno S, Yamano T, et al. Comparison of vascular response after sirolimus-eluting stent implantation between patients with unstable and stable angina pectoris: a serial optical coherence tomography study. JACC Cardiovasc Imaging. 2008;1:475–84.
32. Soeda T, Uemura S, Park S-J, Jang Y, Lee S, Vergallo R, et al. Incidence and Clinical Significance of Poststent Optical Coherence Tomography Findings: One-Year Follow-Up Study From a Multicenter Registry. Circulation. 2015;132:1020–9.
33. Bouma BE, Tearney GJ, Yabushita H, Shishkov M, Kauffman CR, DeJoseph Gauthier D, et al. Evaluation of intracoronary stenting by intravascular optical coherence tomography. Heart. 2003;89: 317–20.
34. Tanigawa J, Barlis P, Dimopoulos K, Dalby M, Moore P, Di Mario C. The influence of strut thickness and cell design on immediate apposition of drug-eluting stents assessed by optical coherence tomography. Int J Cardiol. 2009;134(2):180–8.
35. Fujino Y, Bezerra HF, Attizzani GF, Wang W, Yamamoto H, Chamié D, et al. Frequency-domain optical coherence tomography assessment of unprotected left main coronary artery disease-a comparison with intravascular ultrasound. Catheter Cardiovasc Interv. 2013;82(3):E173–83.
36. Jang IK, Tearney G, Bouma B. Visualization of tissue prolapse between coronary stent struts by optical coherence tomography: comparison with intravascular ultrasound. Circulation. 2001; 104:2754.
37. Kawamori H, Shite J, Shinke T, Otake H, Matsumoto D, Nakagawa M, et al. Natural consequence of post-intervention stent malapposition, thrombus, tissue prolapse, and dissection assessed by optical coherence tomography at mid-term follow-up. Eur Heart J Cardiovascular Imaging. 2013;14(9):865–75.
38. Cook S, Wenaweser P, Togni M, Billinger M, Morger C, Seiler C, et al. Incomplete stent apposition and very late stent thrombosis after drug-eluting stent implantation. Circulation. 2007;115: 2426–34.
39. Sawada T, Shite J, Shinke T, Tanino Y, Ogasawara D, Kawamori H, et al. Very late thrombosis of sirolimus-eluting stent due to late malapposition: serial observations with optical coherence tomography. J Cardiol. 2008;52:290–5.
40. Guagliumi G, Sirbu V, Musumeci G, Gerber R, Biondi-Zoccai G, Ikejima H, et al. Examination of the in vivo mechanisms of late drug-eluting stent thrombosis: findings from optical coherence tomography and intravascular imaging. JACC Cardiovasc Interv. 2012;5:12–20.
41. Gutierrez-Chico JL, Regar E, Nuesch E, Okamura T, Wykrykowska J, di Mario C, Windecker S, van Es GA, et al. Delayed coverage in malapposed and side-branch stents: in vivo assessment with optical coherence tomography. Circulation. 2011;124:612–23.
42. Chamié D, Bezerra HG, Attizzani GF, Yamamoto H, Kanaya T, Stefano GT, et al. Incidence, predictors, morphological characteristics, and clinical outcomes of stent edge dissections detected by optical coherence tomography. JACC Cardiovasc Interv. 2013;6(8):800–13.
43. De Cock D, Bennett J, Ughi GJ, Dubois C, Sinnaeve P, Dhooge J, et al. Healing course of acute vessel wall injury after drug-eluting stent implantation assessed by optical coherence tomography. Eur Heart J Cardiovasc Imaging. 2014;15(7):800–9.
44. Imola F, Occhipinti M, Biondi-Zoccai G, Di Vito L, Ramazzotti V, Manzoli A, et al. Association between proximal stent edge positioning on atherosclerotic plaques containing lipid pools and postprocedural myocardial infarction (from the CLI-POOL Study). Am J Cardiol. 2013;111:526–31.
45. Kim JS, Hong MK, Fan C, Kim TH, Shim JM, Park SM, et al. Intracoronary thrombus formation after drug-eluting stents implantation: optical coherence tomographic study. Am Heart J. 2010;159(2):278–83.
46. Gonzalo N, Serruys PW, Okamura T, van Beusekom HM, Garcia-Garcia HM, von Soest G, et al. Optical coherence tomography patterns of stent restenosis. Am Heart J. 2009;158:284–93.
47. Nagai H, Ishibashi-Ueda H, Fujii K. Histology of highly echolucent regions in optical coherence tomography images from two patients with sirolimus-eluting stent restenosis. Catheter Cardiovasc Interv. 2010;75:961–3.
48. Kume T, Akasaka T, Kawamoto T, Watanabe N, Toyota E, Sukmawan R, et al. Visualization of neointima formation by optical coherence tomography. Heart J. 2005;46:1133–6.
49. Nakazawa G, Otsuka F, Nakano M, Vorpahl M, Yazdani SK, Ladich E, et al. The pathology of neoatherosclerosis in human coronary implants bare-metal and drug-eluting stents. J Am Coll Cardiol. 2011;57(11):1314–22.
50. Takano M, Yamamoto M, Inami S, Murakami D, Ohba T, Seino Y, Mizuno K. Appearance of lipid-laden intima and neovascularization after implantation of bare-metal stents extended late-phase observation by intracoronary optical coherence tomography. J Am Coll Cardiol. 2009;55(1):26–32.
51. Hou J, Qi H, Zhang M, Ma L, Liu H, Han Z, et al. Development of lipid-rich plaque inside bare metal stent: possible mechanism of late stent thrombosis? An optical coherence tomography study. Heart. 2010;96(15):1187–90.
52. Yamaji K, Inoue K, Nakahashi T, Noguchi M, Domei T, Hyodo M, et al. Bare metal stent thrombosis and in-stent neoatherosclerosis. Circulation. 2012;5:47–54.
53. Kim JS, Kato K, Kim SJ, Xing L, Yeh RW, et al. Comparison of incidence and time course of neoatherosclerosis between bare metal stents and drug-eluting stents using optical coherence tomography. Am J Cardiol. 2012;110(7):933–9.
54. Serruys PW, Onuma Y, Dudek D, Smits PC, Koolen J, Chevalier B, et al. Evaluation of the second generation of a bioresorbable everolimus-eluting vascular scaffold for the treatment of de novo

coronary artery stenosis 12-month clinical and imaging outcomes. J Am Coll Cardiol. 2011;58:1578–87.
55. Serruys PW, Ormiston JA, Onuma Y, Regar E, Gonzalo N, Garcia-Garcia HM, et al. A bioabsorbable everolimus-eluting coronary stent system (ABSORB): 2-year outcomes and results from multiple imaging methods. Lancet. 2009;373: 897–910.
56. Bourantas CV, Serruys PW, Nakatani S, Zhang YJ, Farooq V, Diletti R, et al. Bioresorbable vascular scaffold treatment induces the formation of neointimal cap that seals the underlying plaque without compromising the luminal dimensions: a concept based on serial optical coherence tomography data. EuroIntervention. 2015;11:746–56.
57. Okamura T, Onuma Y, Garcia-Garcia HM, Regar E, Wykrzkowska JJ, Koolen J, et al. 3-dimensional optical coherence tomography assessment of jailed side branches by bioresorbable vascular scaffolds: a proposal for classification. J Am Coll Cardiol Intv. 2010;3:836–44.